Use of Microelectrode Arrays To Directly Measure Diffusion of Ions in Solid Electrolytes: Physical Diffusion of Ag^+ in a Solid Polymer Electrolyte

Vince Cammarata, Daniel R. Talham, Richard M. Crooks, and Mark S. Wrighton*

Department of Chemistry, Massachusetts Institute of Technology, Cambridge, Massachusetts 02139
(Received: June 27, 1989)

We report experiments that demonstrate methodology for direct measurement of diffusion of molecular or ionic species in solid electrolyte media. A microelectrode array of closely spaced (1.4-μm) Pt microelectrodes (~70 μm long × 2.7 μm wide × 0.1 μm high) allows direct measurement of the movement of Ag^+ in aqueous electrolyte and in the solid polymer electrolytes, $LiCF_3SO_3$/MEEP [MEEP = poly(bis(2-(2-methoxyethoxy)ethoxy)phosphazene)] at 298 K with a molar ratio of $LiCF_3SO_3$ to polymer repeat unit of 1 to 4 and $LiCF_3SO_3$/PEO [PEO = poly(ethylene oxide)] at 352 K and a molar ratio of $LiCF_3SO_3$ to polymer repeat unit of 1 to 8. The crucial experiments involve anodically stripping Ag from a Ag-coated Pt microelectrode (generator) and electrochemically detecting the resulting Ag^+ at nearby (1.4–23.4-μm) Pt electrodes (collectors) by reducing the Ag^+ back to Ag. The time dependence of the collector current corresponding to Ag^+-to-Ag reduction after the generation step allows evaluation of the diffusion coefficient, D, for the Ag^+ in the various media and conditions used: $D = 5 \pm 2 \times 10^{-9}$ cm²/s at 298 K in $LiCF_3SO_3$/MEEP, $2.3 \pm 0.3 \times 10^{-5}$ cm²/s in aqueous 0.1 M $LiClO_4$, and $7 \pm 1 \times 10^{-8}$ cm²/s at 352 K in $LiCF_3SO_3$/PEO. For the arrays used, $D = 0.22d^2/t_{mt}$ where d is the separation between the generator and the collector and t_{mt} is the time of the maximum collector current.

Introduction

We have recently communicated a technique that allows the electrochemical determination of the diffusion coefficient, D, of a redox-active species by monitoring the time required for a species to move from a "generator" electrode, through an electrolyte medium, to a separate "collector" electrode, Scheme I.[1] The critical measurement is to determine the time dependence of the collector current associated with the redox chemistry of the species created at the generator. Equation 1 has been shown to apply

$$D = 0.22d^2/t_{mt} \quad (1)$$

to a geometry of generator/collector electrodes consisting of parallel microelectrodes where D is the diffusion coefficient of the species created at the generator, d is the distance from the center of the generator to the nearest edge of the collector, and t_{mt} is the time associated with the maximum in the collector current.[1]

In this report we demonstrate the utility of microelectrode generation/collection techniques to directly measure the movement of ions in solid polymer electrolyte media and to determine their diffusion coefficients. The experimental strategy is summarized in Scheme II. The critical measurement is the time dependence of the collector current corresponding to the reduction of Ag^+ after the pulsed generation of Ag^+ from a Ag-coated generator electrode, a distance d from the collector. For simplicity, we assume Ag^+ movement; however, the actual species moving may be Ag^+, $Ag^+CF_3SO_3^-$, $Ag^+(S)$, or $Ag^+CF_3SO_3^-(S)$ where S is one or more solvent molecules. In any case, we detect the movement of some Ag^+ species from one point in space to another.

One new measurement techniques complement studies of ionic conductivity by ac impedance, pulsed-field-gradient NMR, and radio-tracer methods.[2,3] Measurements of solid-state ionic conductivity from ac impedance are not always easily interpreted;[4] however, the measurements here directly provide data concerning diffusivity. Electrochemical studies to determine D based on steady-state currents of codissolved electroactive species have been made in solvent-swollen solid electrolytes.[5] Measurements of the effective diffusion coefficient for charge transport in a redox polymer have been made using a microelectrode array coated with

SCHEME I: Experiment To Measure Diffusivity of Electrogenerated Species Using a Microelectrode Array

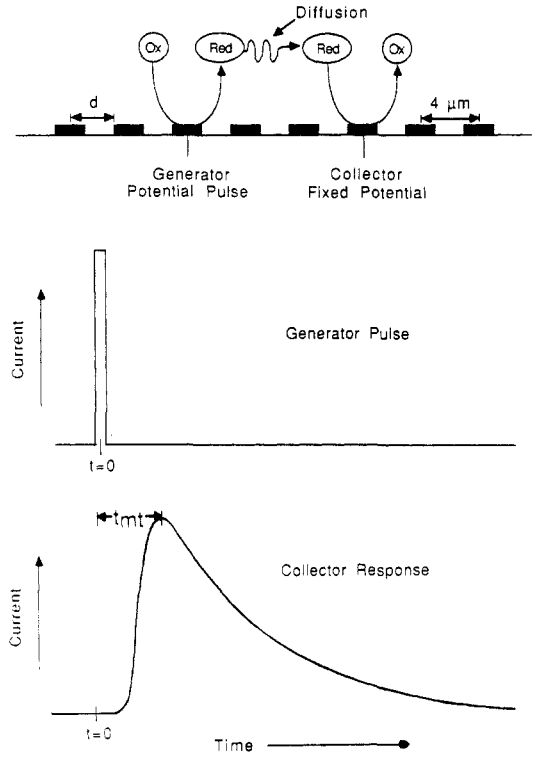

SCHEME II: Experimental Strategy for Ag^+ Transit Time Determination

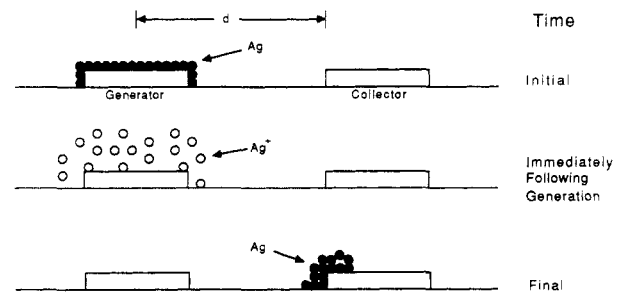

(1) Licht, S.; Cammarata, V.; Wrighton, M. S. *Science* **1989**, *243*, 1176. Licht, S.; Cammarata, V.; Wrighton, M. *J. Phys. Chem.*, in press. Similar transit time techniques have been employed using rotating ring disk electrodes: Prater, K. B.; Bard, A. J. *J. Electrochem. Soc.* **1970**, *117*, 207. Bruckenstein, S.; Miller, B. *Acc. Chem. Res.* **1977**, *10*, 54.
(2) Vincent, C. A. *Prog. Solid State Chem.* **1987**, *17*, 145.
(3) Macdonald, J. R. *Impedance Spectroscopy*; Wiley-Interscience: New York, 1987.
(4) Shriver, D. F.; Ratner, M. A. *Chem. Rev.* **1988**, *88*, 109.

0022-3654/90/2094-2680$02.50/0

SCHEME III: Structures of MEEP and PEO

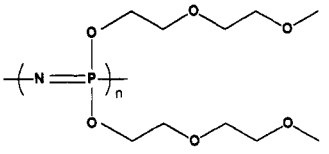

Poly[bis(2-(2-methoxyethoxy)ethoxy)phosphazene]

MEEP

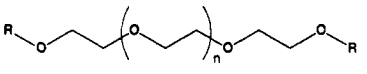

Poly(ethylene oxide)

PEO

a polymer.[6,7] In the redox polymer studies, the movement of charge is a diffusion process that occurs via electron hopping, driven by a concentration gradient between oxidized and reduced sites. Our extension of this methodology relates to a situation where net physical movement of an ion occurs in a nonelectronic conductive media. A significant point regarding our method for determining D for Ag^+ is that the measurement is unambiguous in terms of the movement of the Ag^+, because all the Ag is initially confined to the generator and the current measured is due to the reduction only at the collectors. Transit-time techniques can determine diffusion coefficients without knowledge of the concentration of the diffusing species.[6]

Solid electrolytes show great promise in battery technology, in solar energy systems, and in solid-state gas sensors.[8] Solid polymer electrolytes differ from the classical solid electrolytes in that generally they are conductive in the elastomeric phase as opposed to in a crystalline or polycrystalline phase. Since they are generally glasses at operating temperature, embrittlement and delamination do not limit long-term durability.

Processing these materials for the construction of odd shapes or sizes is facilitated by their plasticity. Many ionic conducting polymers behave as solvents for ions that have, on a microscopic scale, liquid-like degrees of freedom. Our primary illustration of the direct dynamic movement of ions through a solid concerns the solid electrolyte, MEEP/$LiCF_3SO_3$ at a 1 to 4 molar ratio of $LiCF_3SO_3$ to polymer repeat unit.[9] MEEP, shown in Scheme III, is known to have good ionic conductivity for many monovalent salts at 298 K.[10] We have also studied PEO/$LiCF_3SO_3$ at a 8 to 1 molar ratio of polymer repeat unit to $LiCF_3SO_3$.[11] PEO, also shown in Scheme III, has good ionic conductivity above the melting point of the crystalline phase (~67 °C) and is the most well studied of the organic polymer solid electrolytes.[2,12] The structure of both of these polymers include ether linkages separated by $-CH_2CH_2-$ groups analogous to crown ethers and their linear analogues. The affinity of this class of molecules for alkali-metal cations is well documented.[2,4] The mechanism of conduction (diffusion) is assumed to be ion hopping from Lewis base site to Lewis base site in which chain motion is a significant factor.[13] This is inferred from discontinuities in the conductivity–temperature plots near the melting point of these polymers. Our studies provide some of the first data on direct measurement of diffusivity of ions in solid polymer electrolytes. The methodology can be applied to studies to investigate the factors governing ionic conductivity.

Experimental Section

Materials. The polymers PEO and MEEP were deposited from 1–2% stock solutions based on CH_3CN and tetrahydrofuran (THF), respectively (i.e., 100-mg MEEP/10-mL THF). PEO (Aldrich, MW 5×10^6) was dried under 1-mmHg vacuum at 50 °C for 24 h and then stored in a Vacuum Atmospheres drybox for later use. $LiCF_3SO_3$ (Aldrich) was dried at 100 °C for 24 h under vacuum. MEEP[9,10] was a generous gift from Professor H. R. Allcock at the Pennsylvania State University. The polymers were dissolved in CH_3CN or THF with 4:1 and 8:1 molar ratios of polymer repeat unit to electrolyte for MEEP and PEO, respectively. Solvents used were reagent grade and were distilled from CaH_2 before use.

Microelectrode Modification. The Pt microelectrode arrays used have been described previously[14] and consist of eight, individually addressable Pt microelectrodes each 70 μm long × 2.7 μm wide × 0.1 μm high with an interelectrode spacing of 1.4 μm. A small area of Ag epoxy was placed 300–500 μm from the array to be used as a counterelectrode in these experiments. Ag metal was then deposited on the characterized array. At least one electrode typically no. 1 or 8 was plated with Ag metal to act as a reference electrode under the solid electrolyte. Ag metal was selectively deposited by pulsing the desired electrodes from 0 to −0.5 V vs Ag wire in a commercial silver cyanide plating bath (Transene Co.) for 1–2 s. The remaining electrodes were held at +0.2 V vs Ag wire. Typical plating currents were 50–200 nA/electrode (~10 mA/cm²). Typical Ag coverage was $\sim 10^{-8}$ mol/cm², cf. Figure 2. The Ag-coated microelectrode array devices were brought into the drybox, and 1 or 2 drops of polymer solution were placed on the electrode surface. The devices were then placed in the antechamber of the drybox and dried by slowly evacuating the antechamber to an ultimate vacuum of 0.1 mmHg over 15 min. The devices were left under vacuum for an additional 1.5 h. The device was then brought back into the drybox and fitted through a rubber septum into a round-bottom flask in order to maintain an inert atmosphere above the device throughout the experiment. An amount of 20 μL of THF per 50 mL of N_2 atmosphere was injected as a "plasticizer" to increase ionic conductivity[2,4,5] and to ensure a reproducible atmosphere. PEO experiments were done at elevated temperatures above the melting point (~67 °C) of the polymer while the MEEP experiments were done at room temperature (~23 °C).

Characterization Techniques. Auger electron spectra were obtained on a Physical Electronics Model 660 scanning auger microprobe. Scanning electron micrographs were obtained on a Hitachi Model 5 800 instrument. Optical photography was taken on a Bausch and Lomb MicroZoom microscope.

Electrochemical Measurements. Electrochemical equipment consisted of a Pine Instruments Model RDE4 bipotentiostat with special modification to include a 100 nA/V scale and with leads prior to the first-stage amplifier shielded to the chassis ground. The electrochemical cell was enclosed by a Faraday shield or in the high-temperature experiments enclosed in a Will lab oven to stabilize the operating temperature. Signals were recorded on Kipp and Zonen Model BD 91 X-Y-Y′ dual-pen chart recorder or dual-channel Nicolet Model 4904 digital collection oscilloscope.

(5) Reed, R. A.; Geng, L.; Murray, R. W. *J. Electroanal. Chem. Interfacial Electrochem.* **1986**, *208*, 185. Geng, L.; Reed, R. A.; Longmire, M.; Murray, R. W. *J. Phys. Chem.* **1987**, *91*, 2908. Geng, L.; Longmire, M. L.; Reed, R. A.; Parcher, J. F.; Barbour, C. J.; Murray, R. W. *Chem. Mater.* **1989**, *1*, 58. Geng, L.; Reed, R. A.; Kim, M.-H.; Wooster, T. T.; Oliver, B. N.; Egekeze, J.; Kennedy, R. T.; Jorgenson, J. W.; Parcher, J. F.; Murray, R. W. *J. Am. Chem. Soc.* **1989**, *111*, 1614.

(6) Feldman, B. J.; Feldberg, S. W.; Murray, R. *J. Phys. Chem.* **1987**, *91*, 6558.

(7) Kittlesen, G. P.; White, H. S.; Wrighton, M. S. *J. Am. Chem. Soc.* **1985**, *107*, 7373. Smith, D. K.; Lane, G. A.; Wrighton, M. S. *J. Am. Chem. Soc.* **1986**, *108*, 3522. Belanger, D.; Wrighton, M. S. *Anal. Chem.* **1987**, *59*, 1426.

(8) Chiang, C. K. *Polymer* **1981**, *22*, 1454. Skotheim, T. A.; Lundstrom, I. *J. Electrochem. Soc.* **1982**, *129*, 894. Chao, S.; Wrighton, M. S. *J. Am. Chem. Soc.* **1987**, *109*, 8.

(9) Allcock, H. R.; Austin, P. E.; Neenan, T. X.; Sisko, J. T.; Blonsky, P. M.; Shriver, D. F. *Macromolecules* **1986**, *19*, 1508. Austin, P. E.; Riding, G. H.; Allcock, H. R. *Macromolecules* **1983**, *16*, 719.

(10) Blonsky, P. M.; Shriver, D. F.; Austin, P. E.; Allcock, H. R. *J. Am. Chem. Soc.* **1984**, *106*, 6854. Blonsky, P. M.; Shriver, D. F.; Austin, P. E.; Allcock, H. R. *Solid State Ionics* **1986**, *18*, 258.

(11) Weston, J. E.; Steele, B. C. H. *Solid State Ionics* **1981**, *2*, 347.

(12) Armand, M. B.; Chabagno, J. M.; Duclot, M. J. In *Fast Ion Transport in Solids*; Vashishta, P., Mundy, J. N., Shenoy, G. K., Eds.; North-Holland: Amsterdam, 1979; p 131.

(13) Ratner, M. A. In *Polymer Electrolyte Reviews*; MacCallum, J. R., Vincent, C. A., Eds.; Elsevier: New York, 1987; p 173.

(14) Thackeray, J. W.; White, H. S.; Wrighton, M. S. *J. Phys. Chem.* **1985**, *89*, 5133.

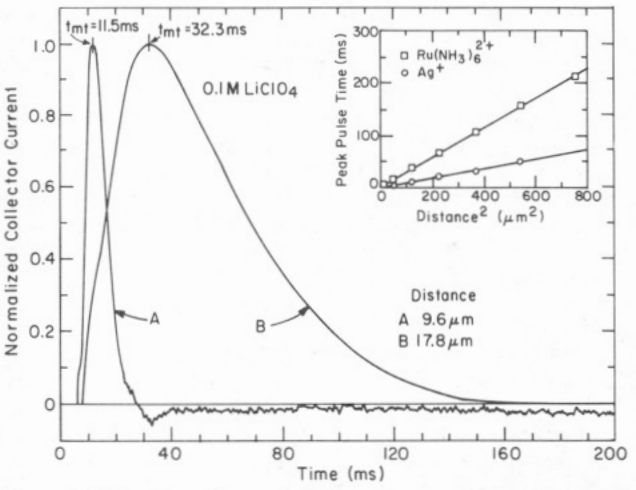

Figure 1. Microelectrode transit time measurements of Ag^+ in 0.1 M $LiClO_4$ aqueous solution. (A) Normalized collector current vs time associated with the reduction of Ag^+ generated by a 2-ms pulse from 0.0 to 1.4 V returning to 0.0 V vs SCE at a Pt generator microelectrode coated with 2×10^{-12} mol of Ag metal separated from the collector by 9.6 μm. The Pt collector microelectrode is held at 0.0 V vs SCE. (B) Normalized collector current vs time associated with a 10-ms anodic pulse under the same conditions as in A with the exception that the interelectrode separation is 17.8 μm. The inset shows the distance dependence of the time of the peak collection current at different collector electrodes for Ag^+ in 0.1 M in $LiClO_4$ and also for $Ru(NH_3)_6^{2+}$ in 0.1 M $NaClO_4$.

Pulses were generated from a Princeton Applied Research Model PAR 175 universal programmer. The Ag^+ solution experiment was performed in an aqueous 0.1 M $LiClO_4$ solution at 23 °C.

Results and Discussion

Diffusion in Liquid Electrolytes. Figure 1 illustrates microelectrode transit time data recorded in aqueous 0.1 M $LiClO_4$ at 298 K. With reference to Scheme I, normalized collection current vs time is shown for two values of d, 9.6 and 17.8 μm, giving values of t_{mt} of 11.5 and 32.3 ms, respectively, for the Ag^+ experiment. Consistent with a diffusion process, the value of t_{mt} is found *experimentally* to be proportional to d^2 as illustrated in the inset of Figure 1. In the Ag^+ experiments only a fraction of the Ag is stripped from the generator. Some Ag is replated on the generator, and the effect on t_{mt} is not significant. The inset of Figure 1 also gives t_{mt} vs d^2 for experiments involving the diffusion of $Ru(NH_3)_6^{2+}$ where the $Ru(NH_3)_6^{2+}$ is generated by reduction of $Ru(NH_3)_6^{3+}$ at the generator.[1] The ratio of slopes of the plots of t_{mt} vs d^2 for the Ag^+ and $Ru(NH_3)_6^{2+}$ gives the ratio of D for these two species, and eq 1 can be used to determine D. Our measurements give $D = 2.3 \times 10^{-5}$ and 7.8×10^{-6} cm^2/s for Ag^+ and $Ru(NH_3)_6^{2+}$, respectively,[15,16] results that agree well with previous measurements. The Ag^+ transit time experiment is somewhat different than the solution species experiment since the generation step involves stripping of confined redox material instead of generation from a solution species. In addition, the collection step truly collects the material at the electrode as opposed to collection being a change in redox state of a solution species. The Ag^+ experiments show that despite the differences in the nature of the redox process, the diffusion of the solution species determines the transit time and the shape of the collection curve.

Surface Analysis. In earlier work on monitoring the diffusion of solution species, it was determined that the best fit of the distance dependence to transit time used to center-to-edge distance on the microelectrode array.[1] Since the generator and collector electrodes have a finite width relative to the gap, it was unclear how far the majority of the species had to travel. Although this empirical formula worked well in the cases considered, direct experimental evidence justifying its use was lacking. Optical microscopy of an array after a Ag^+ microelectrode transit time experiment in aqueous solution or in MEEP/$LiCF_3SO_3$ (vide infra) shows a dark precipitate on the collector electrodes on the

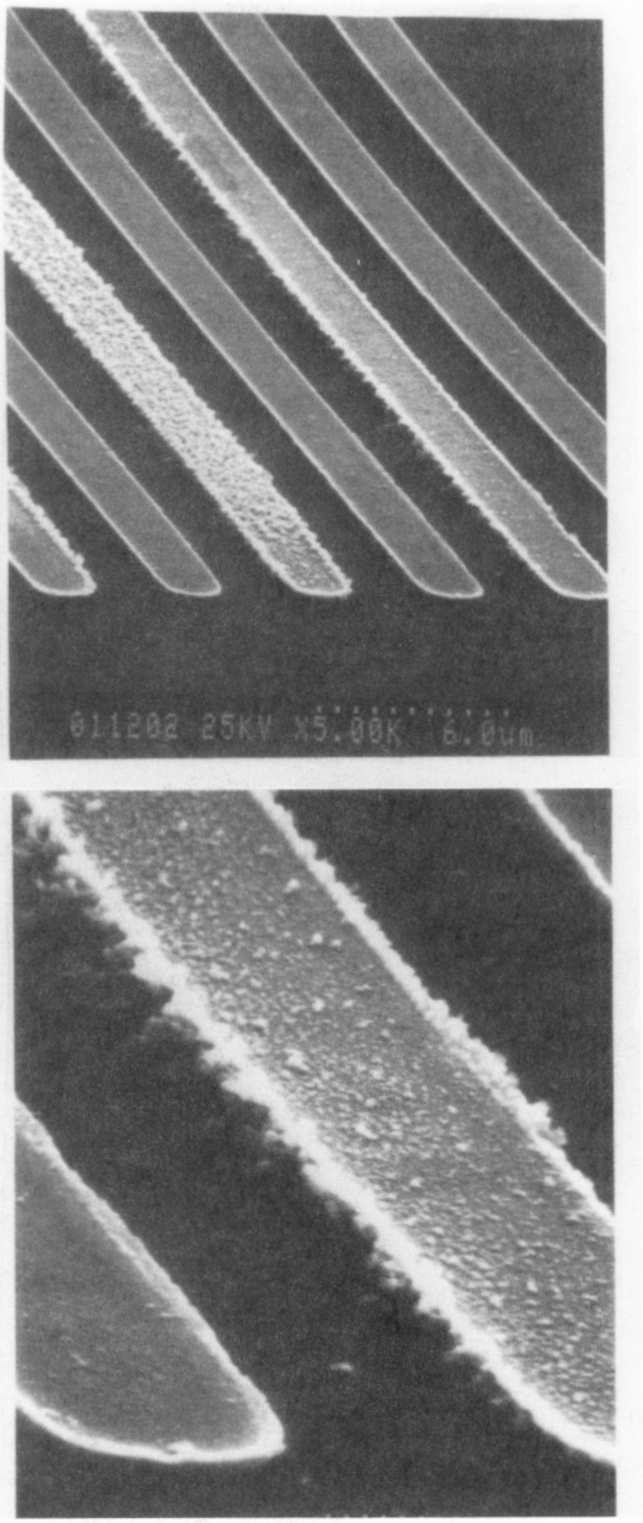

Figure 2. Scanning electron micrographs of a Pt microelectrode array consisting of eight electrodes (each 70 μm long × 2.7 μm wide × 0.1 μm high with an interelectrode spacing of 1.4 μm). Ag (5×10^{-13} mol) was deposited on electrode no. 4 (electrodes are numbered 1–8, left to right, see Experimental Section) and then stripped by pulsing from −0.6 to 1.2 V vs SCE three times for 10 ms each in an aqueous 0.1 M $LiClO_4$. The collector electrodes, no. 2 and no. 6, were held at −0.6 V. The rest of the microelectrode array was left "floating" (i.e., not under potentiostatic control). (Upper) Electrodes no. 2–8 are shown. (Lower) Electrodes no. 5 and no. 6 are shown closeup.

(15) von Stackelberg, M.; Pilgram, M.; Toome, W. *Z. Elektrochem.* **1953**, *57*, 342.

(16) D for $Ru(NH_3)_6^{2+}$ has been independently measured at a 25-μm microdisk electrode from the limiting steady-state currents.

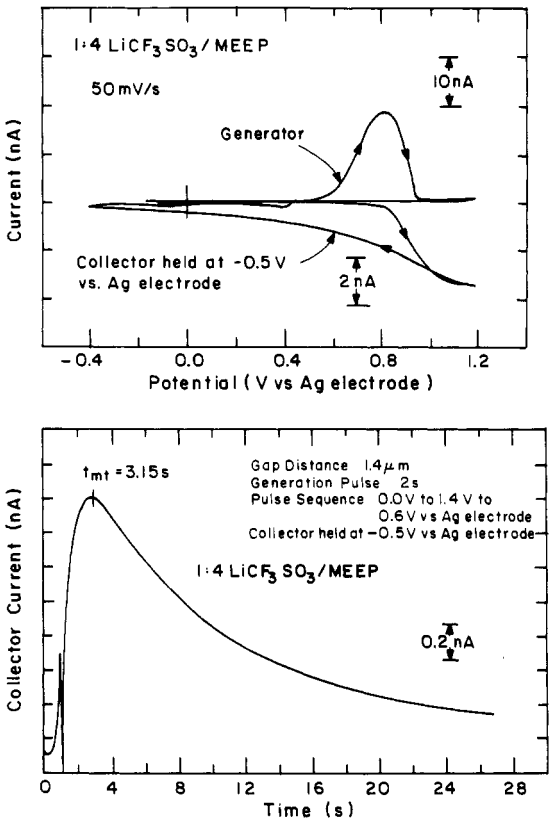

Figure 3. (Upper) Generation/collection voltammograms of Ag^+ in 1:4 $LiCF_3SO_3$/repeat unit of MEEP. The generator microelectrode was scanned from −0.5 to 1.2 V vs Ag quasi-reference electrode at 50 mV/s. Dual collector electrodes are symmetrically disposed about the generator and are 1.4 μm away from the generator. The collector electrodes were held at −0.5 V vs Ag. (Lower) Collector current vs time associated with the reduction of Ag^+ generated with a 2-s step of the Ag-coated Pt generator to +1.4 V and back to +0.6 V vs Ag in the same $LiCF_3SO_3$/MEEP electrolyte.

nearest edge to the generator. This is diagrammed in Scheme II. Figure 2 shows a scanning electron micrograph (SEM) of a Pt array on which 5×10^{-8} C of Ag was deposited on electrode no. 4 then anodically stripped by pulsing from −0.6 to +1.2 V vs SCE in an aqueous 0.1 M $LiClO_4$ solution. The collector electrodes, no. 2 and no. 6 (the second electrodes away), are held at −0.6 V vs SCE. In the SEM, the deposition of the dark precipitate is confirmed and the extent of the localization on the collector electrode is shown. Auger analyses confirm that the black precipitate on the collector electrodes and the generator is indeed Ag. The Auger analysis also confirms that Ag is deposited mainly on the edge of the collector electrode nearest the generator and not on the center or far edge or at electrodes not used as collectors. Since Ag is initially confined to the generator electrode and after the experiment localized on the closest edge of the collector electrodes, Ag travels from generator to the edge of the collector.

Diffusion in Solid Electrolytes. The top portion of Figure 3 shows the generation/collection voltammograms for Ag^+ in MEEP/$LiCF_3SO_3$. The anodic curve represents the stripping voltammogram for Ag by scanning the Ag-coated Pt electrode from −0.5 to +1.4 V vs Ag electrode at 50 mV/s. The cathodic curve is the current for Ag^+ reduction monitored concurrently at two collector electrodes, symmetrically disposed 1.4 μm from the generator and held at −0.5 V vs Ag quasi-reference electrode. Subsequent stripping analysis of the collector electrode confirms that the product deposited there is Ag. This result shows that Ag^+ indeed travels from the generator to the collector electrodes in the polymer electrolyte.

The lower portion of Figure 3 shows the microelectrode transit time experiment in MEEP/$LiCF_3SO_3$. The collector current peak of 2.2 nA occurs at 3.15 s for the generation conditions used. Comparing the time for the maximum in collector current in

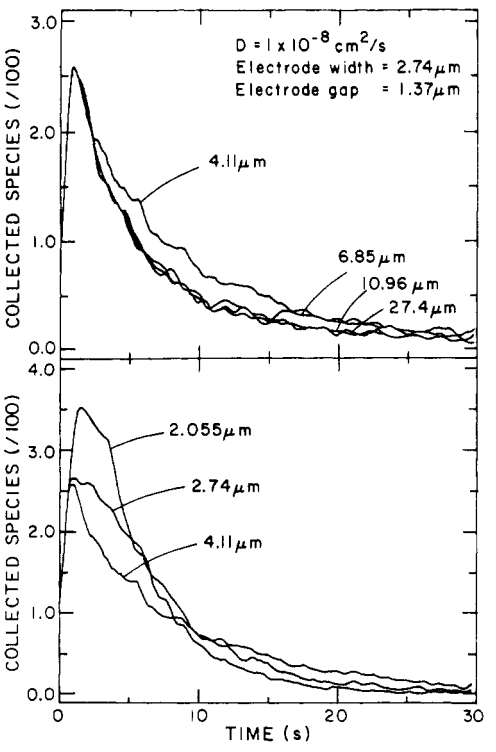

Figure 4. Time vs collection flux shown for various reflective boundary conditions in a random-walk simulation. The diffusion coefficient was taken to be 1×10^{-8} cm^2/s. (Upper) The reflective boundaries are taken as 27.4, 10.96, 6.85, and 4.11 μm from the generator. (Lower) The reflective boundaries are taken as 4.11, 2.74, and 2.055 μm from the generator.

aqueous 0.1 M $LiClO_4$ and $LiCF_3SO_3$/MEEP shows that the peak occurs ~3000 times later in the solid electrolyte and $D = 5 \times 10^{-9}$ cm^2/s. The shape of the collector current vs time plot (adjusted for height and width) is similar in both solid and liquid experiments to measure the diffusivity of Ag^+.

Transit time experiments have also been done in PEO/$LiCF_3SO_3$ media at 352 K. From experiments similar to those described above, we find t_{mt} = 240 ms. With use of eq 1, $D = 7 \times 10^{-8}$ cm^2/s in this system.

Computer Simulations. Earlier work on redox-active ions in solution included simulating the microelectrode transit time experiment.[1] In those cases, a semiinfinite boundary condition could be applied since the solution volume dimensions were greater than the critical diffusion lengths. We estimate polymer thickness to exceed 10 μm, but our studies lack accurate information on polymer thicknesses. Surface profilometry yields little information (the stylus cuts through the polymer), and the lack of density information on MEEP (solvent swollen or dry) and the irregularity of the area over which the polymer is spread also contribute to this information gap. To get a better perspective on the dependency of transit time on polymer thickness, digital simulations of such experiments were performed. The simulation is similar to that of the solution case with two exceptions.[1] First, the spatial resolution of the basis grid is more sensitive (i.e., 0.685- vs 1.37-μm spacing for our 1.37-μm gap devices). Second, the boundary conditions are changed such that a reflective boundary is placed at a given distance from the array surface. This replaces the semiinfinite boundary of the solution simulation. The boundary is intended to model the interface of the polymer with the atmosphere. This boundary is adjustable so that the collector response as a function of time can be simulated as a function of film thickness. The diffusing species is given a simulated diffusion coefficient of 1×10^{-8} cm^2/s.

The plot of the flux of collected species as a function of time is relevant to the observed experimental results (collector current vs time) in the transit time experiments. Figure 4 shows the flux of collected species as a function of time for a number of simulated polymer thicknesses at a microelectrode array with symmetric,

adjacent collectors. The simulation is of long, parallel, microelectrodes (2.74 μm wide) spaced 1.37 μm apart assuming release of Ag^+ in a step from a central generator flanked by two collectors. The top portion of this figure shows the flux profiles as a function of time for thicknesses of 27.4, 10.96, 6.85, and 4.11 μm. For 27.4- and 10.96-μm thicknesses, the collection vs time curves are identical. In the 6.85-μm case, the flux profile shows increased collection around 15 s but the peak flux remains unchanged. At the 4.11-μm thickness, the peak starts to broaden, and below this limit, the simulation shows significant differences from the semiinfinite case. This seems reasonable since the species would have to reach the boundary and return to the collector before the information relating to the thickness would be transmitted to the collector. Only when the thickness is on the order of the interelectrode spacing does the boundary condition affect the microelectrode transit time results. The lower portion of Figure 4 shows the collection fluxes vs time for boundary conditions of 2.055 and 2.74 μm as well as 4.11 μm for reference. The peak in the collection flux for the two conditions is severely distorted, though transit time measurements only change ~50% at most. This shows that only measurements with very thin films (less than the interelectrode spacing) would be subject to errors in our analysis of D.

Conclusion

Our results support the conclusion that microelectrochemical techniques can be useful in studies of physical diffusion in solid electrolytes. Results for the movement of Ag^+ in MEEP and PEO establish a methodology, but do not yet provide unambiguous conclusions regarding the actual diffusing species. Additional research will be required to establish details of the diffusion mechanism in solid polymer electrolytes, using microelectrochemical methods. For a given system it is clear that meaningful information will result from measurements of t_{mt} as a function of temperature, electrolyte and its concentration, and the actual polymer used. The values of D reported herein show, as expected, that diffusion of Ag^+ is much slower ($\sim 10^3$) in MEEP or PEO than in aqueous solution. Additional microelectrochemical studies are in progress to investigate the factors influencing the diffusion of metal cations, and new experimental methods are being developed for the study of both anionic and neutral species.

Acknowledgment. We thank Professor H. R. Allcock of the Pennsylvania State University for providing a sample of MEEP. We thank J. J. Hickman for obtaining the Auger analysis and T. J. Gardner for obtaining the scanning electron micrographs. We acknowledge Lockheed Missile and Space Company, Inc., and the Office of Naval Research and the Defense Advanced Research Projects Agency for partial financial support of this research.

Registry No. MEEP, 98973-15-0; PEO, 25322-68-3; Ag^+, 14701-21-4; Pt, 7440-06-4; $LiCF_3SO_3$, 33454-82-9.

Proton Acidity and Chemical Reactivity in Molten Salt Hydrates

S. K. Franzyshen, M. D. Schiavelli,* K. D. Stocker,

Department of Chemistry, College of William and Mary, Williamsburg, Virginia 23185

and M. D. Ingram*

Department of Chemistry, University of Aberdeen, Aberdeen AB9 2UE, Scotland, U.K.
(Received: July 3, 1989)

Molten $Ca(NO_3)_2 \cdot 4H_2O$ has been used as a model system for studies of proton acidity and chemical reactions (including ester hydrolyses and aromatic nitrations) in molten salt hydrates. Increases in proton acidity caused by addition of acidic hydrates such as $AlCl_3 \cdot 6H_2O$ and $Cd(NO_3)_2 \cdot 4H_2O$ or of aqueous HNO_3 can be quantified in terms of changes in Hammett acidity H_0, but usually not by the downfield shifts observed in the NMR spectrum. The rates of hydrolysis of selected primary esters (e.g., *n*-octyl acetate) were found to be linearly dependent on nitric acid concentration, indicating that the acidity of these melts can be changed with little change in water activity. The measurement of kinetic parameters is complicated, however, by side reactions between the organic substrates and HNO_2, NO_2 (or NO_2^+), and other species originating from the nitrate ions in the melt.

Introduction

Molten salt hydrates[1-4] have long been used for modeling the properties of anhydrous fused salts and have highlighted the influence of ionic interactions and melt structure on physical properties. Careful measurements of conductivity and viscosity in mixed $NaNO_3$–KNO_3–$Ca(NO_3)_2 \cdot 4H_2O$ melts[4] and in related systems,[5-7] for example, have provided useful insights into the mechanism of the "mixed alkali-metal effect" which is important in many inorganic glass-forming systems. Nevertheless, despite some remarkable observations, most notably that molten mixtures of $Al(NO_3)_3 \cdot 10H_2O$ and $AlCl_3 \cdot 10H_2O$ attack noble metals more rapidly than does boiling aqua regia,[8] there have been few attempts to explore systematically the reactivity of these media in relation to other properties such as melt acidity.

Evidence for the existence of significant levels of proton acidity in hydrate melts comes from ^1H NMR shifts[8] and, more recently, from measurements of Hammett acidity using organic indicators.[9-11] Angell and co-workers[8] attributed the large downfield shifts (δ_H) observed in melts containing hydrated Al^{3+} ions to

* To whom correspondence should be addressed.

(1) Angell, C. A. *J. Electrochem. Soc.* **1965**, *112*, 1224.
(2) Moynihan, C. T.; Fratiello, A. *J. Am. Chem. Soc.* **1967**, *89*, 5546.
(3) Moynihan, C. T.; Smalley, C. R.; Angell, C. A.; Sare, E. J. *J. Phys. Chem.* **1969**, *73*, 2287.
(4) Moynihan, C. T. *J. Electrochem. Soc.* **1979**, *126*, 2144.
(5) Ingram, M. D.; King, K.; Kranbuehl, D. *J. Phys. Chem.* **1981**, *85*, 289.
(6) Mahiuddin, S.; Ismail, K. *J. Phys. Chem.* **1984**, *88*, 1027.
(7) Sangma, P.; Mahiuddin, S.; Ismail, K. *J. Phys. Chem.* **1984**, *88*, 2378.
(8) Sare, E. J.; Moynihan, C. T.; Angell, C. A. *J. Phys. Chem.* **1973**, *77*, 1869.
(9) Duffy, J. A.; Ingram, M. D. *Inorg. Chem.* **1977**, *16*, 2988; **1978**, *17*, 2798.
(10) Duffy, J. A.; Ingram, M. D. In *Ionic Liquids*; Inman, D., Lovering, D., Eds.; Plenum Press: New York, 1981.
(11) Dyer, R. D.; Fronko, R. M.; Schiavelli, M. D.; Ingram, M. D. *J. Phys. Chem.* **1980**, *84*, 2338.

0022-3654/90/2094-2684$02.50/0